

Article

Reservoir Characteristics of Tight Sandstone and Sweet Spot Prediction of Dibei Gas Field in Eastern Kuqa Depression, Northwest China

Guangjie Zhao ^{1,2}, Xianqing Li ^{1,2,*}, Mancang Liu ³, Caiyuan Dong ³, Daye Chen ⁴ and Jizhen Zhang ^{5,6}

¹ State Key Laboratory of Coal Resources and Safe Mining, China University of Mining and Technology (Beijing), Beijing 100083, China; zhaoguangjie23@126.com

² College of Geoscience and Surveying Engineering, China University of Mining and Technology (Beijing), Beijing 100083, China

³ Research Institute of Petroleum Exploration and Development, PetroChina, Beijing 100083, China; mcliu1970@163.com (M.L.); d1404320223@126.com (C.D.)

⁴ China Coal Research Institute, Beijing 100013, China; chendaye@mail.ccri.ccteg.cn

⁵ Key Laboratory of Exploration Technologies for Oil and Gas Resources, Ministry of Education, Yangtze University, Wuhan 430100, China; zhangjz1991@126.com

⁶ College of Resources and Environment, Yangtze University, Wuhan 430100, China

* Correspondence: lixq@cumtb.edu.cn



Citation: Zhao, G.; Li, X.; Liu, M.; Dong, C.; Chen, D.; Zhang, J. Reservoir Characteristics of Tight Sandstone and Sweet Spot Prediction of Dibei Gas Field in Eastern Kuqa Depression, Northwest China. *Energies* **2022**, *15*, 3135. <https://doi.org/10.3390/en15093135>

Academic Editors: Mofazzal Hossain, Hisham Khaled Ben Mahmud and Md Motiur Rahman

Received: 17 March 2022

Accepted: 21 April 2022

Published: 25 April 2022

Publisher's Note: MDPI stays neutral with regard to jurisdictional claims in published maps and institutional affiliations.



Copyright: © 2022 by the authors. Licensee MDPI, Basel, Switzerland. This article is an open access article distributed under the terms and conditions of the Creative Commons Attribution (CC BY) license (<https://creativecommons.org/licenses/by/4.0/>).

Abstract: Great progress has been made in the exploration of tight sandstone gas resources in Kuqa depression. Great progress has been made in Dibei structural belt, which proves the previously unproven favorable area for tight sandstone gas. The physical properties, controlling factors, and characteristics of tight sandstone from the Ahe (J₁a) Formation in the Dibei gas reservoir are analyzed. The results show that the tight sandstone of the J₁a Formation is mainly feldspar lithic sandstone, with low porosity (average 9.1%) and low permeability (average 0.09 mD). Compaction (average compaction rate 61.9%) reduces porosity more than cementation (average cementation rate 14.3%). Secondary dissolution pores (average thin section porosity is 3.4%) dominate. The homogenization temperature has two peaks; the first peak is 85–110 °C, and the other peak is 115–140 °C, indicating that oil and gas experienced two filling stages at 12 Ma and 4.5 Ma, respectively. Eodiagenesis, A substage of mesogenetic diagenesis, and B substage of mesogenetic diagenesis happened in the area. Tight sandstone is developed in the B substage of mesogenetic diagenesis. The main controlling factors of diagenesis are: strong dissolution and structural pore increase; oil and gas charging and overpressure. The reservoir forming mode of the Dibei gas reservoir is: crude oil filling in the Late Neogene (12 Ma); reservoir densification in the late deposition of Kangcun Formation (7 Ma), mature natural gas filling in the early deposition of Kuqa Formation (4.5 Ma), and gas reservoir formed after transformation and adjustment in the deposition period of Quaternary (2 Ma). According to this model, it is predicted that the favorable area of the Dibei gas reservoir is in the southeast of the Yinan 2 well. This study provides guidance for the study of tight sandstone gas in other areas of the Kuqa Depression.

Keywords: diagenetic evolution; sweet spot; tight sandstone reservoir; controlling factors; Dibei gas field; Kuqa depression

1. Introduction

With the advancement of oil and gas exploration, unconventional oil and gas have become an attractive subject [1–4]. Tight gas is an unconventional natural gas resource with huge reserves in many countries around the world, such as China, the United States, Canada, Russia, Europe, and Saudi Arabia in the Middle East [4–9]. Tight sandstone reservoirs were discovered in China's Tarim, Sichuan, Ordos Basin, Songliao, and Bohai Bay Basin, and great achievement has been made [10–14]. The favorable exploration area

of tight oil in these basins is $16 \times 10^4 \text{ km}^2$, and the oil geological resources are about $(160\text{--}200) \times 10^8 \text{ t}$ [15].

The Dibei tight gas field is large and is discovered deep in the Jurassic in the Kuqa depression [16]. By contrast, the Dina, Dabei, Keshen, and other large tight gas fields are located in the Cretaceous and Eocene layers [17–19]. The reserves report provided by the PetroChina Tarim Oilfield (PCTO) predicts that the reserve of the Dibei gas field is $1.64 \times 10^{11} \text{ m}^3$ [16]. Moreover, compared with other gas fields in the depression, the distribution of gas and water in the area is irregular [16]. Therefore, studying the sweet spot prediction and accumulation mode of the Dibei gas field is beneficial to provide a basis for the deep Jurassic tight gas exploration in the basin. There are a lot of natural gas and a little liquid hydrocarbon in the Dibei gas reservoir. The Jurassic Ahe Formation (J_{1a}) has a commercial-grade gas layer, and the overlying Lower Jurassic Yangxia Formation (J_{1y}) has a poor gas layer [20].

The sandstone reservoir of the J_{1a} Formation is a typical tight reservoir with poor porosity and permeability and high pore pressure [21]. In order to explore the formation mechanism of relatively high-quality reservoirs, many studies have been carried out [16,22–24]. Diagenesis is a key geological process that affects reservoir quality [25,26]. However, the development of good-quality tight sandstones in different oil and gas basins is affected by different diagenesis [27–29]. Therefore, the influence of diagenesis needs to be further studied. The tight sandstone of the J_{1a} Formation has strong heterogeneity [22], which provides a useful example for researching the changes of tight sandstone diagenesis. In addition, studying the process of diagenesis provides a basis for the development of good-quality tight sandstones.

The research objectives are as follows: (a) to study in detail the physical characteristics (composition, structural pore system, physical properties, and diagenetic minerals) of the J_{1a} tight sandstone; (b) to reveal the types, characteristics, and diagenetic stages of diagenesis; (c) to reveal the controlling factors of tight sandstone reservoir; (d) to establish the accumulation mode of tight sandstone gas reservoirs and point out favorable sweet spots. The result provides a scientific basis for other tight sandstone reservoirs in the Kuqa depression and other areas.

2. Geological Setting

Kuqa depression is in the northern Tarim Basin, which is adjacent to the Tianshan fold belt in the north [30] (Figure 1). It is a Mesozoic–Cenozoic foreland basin, which developed in the late Hercynian, and the superposition of multiple tectonic movements occurred, such as the extension depression stage during Jurassic–Paleogene and the development stage of intracontinental foreland thrust during Neogene–Quaternary [31]. It includes eight secondary structural units, including four structural belts: Northern monoclinial, Kelasu, Yiqikelike, Qiulitage, and Southern slope belt as well as three sags: Baicheng, Yangxia, and Wushi Sag [32,33].

There are sedimentary strata in Kuqa depression: Triassic, Jurassic, Cretaceous, Paleogene, and Quaternary sediments [34]. Source rocks in the area mainly include lacustrine mudstones in the Triassic and the coal seams, carbonaceous mudstone, and lacustrine mudstone in the Jurassic [35] (Figure 2). The favorable reservoirs comprise J_{1a} and J_{1y} Formation in Jurassic, Cretaceous Bashijiqike (K_{1bs}), Suweiyi (E_{3s}), and bottom conglomerate of Kumugeliemu (E_{1-2} km) in Paleogene, Jidike (N_{1j}) Formation in Neogene. The cap rocks of Jurassic and Cretaceous strata in Mesozoic are mainly mudstone, which is widely distributed throughout the depression. The Neozoic cap rocks are mainly in the E_{1-2} km and the N_{1j} strata, which mainly include the gypsum and salt layers.

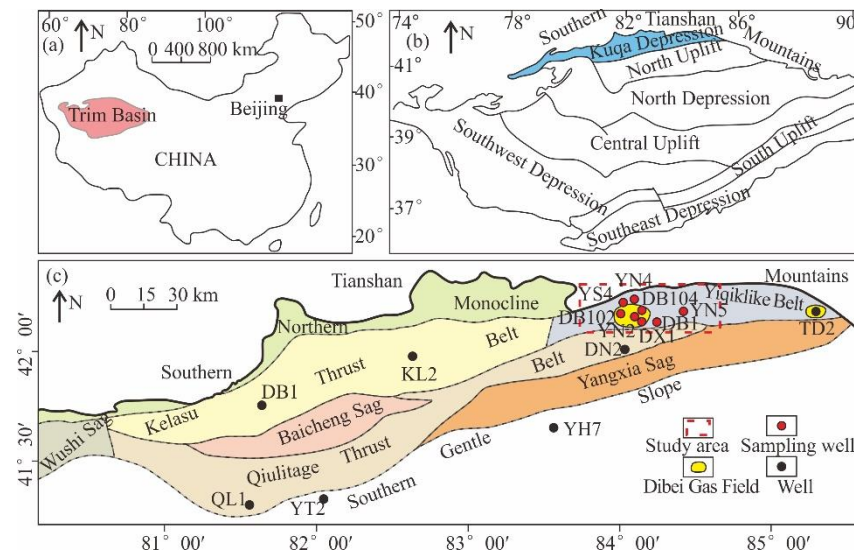


Figure 1. Tectonic units and location of Dibeï gas field in Kuqa Depression. (a) Location of Tarim Basin; (b) location of Kuqa Depression; (c) sample wells and structural outline of Dibeï gas field in Kuqa Depression.

Stratigraphy					Lithology	Thick-ness (m)	Source Rock	Reservoir Rock	Cap Rock	Age (Ma)	Tectonic Movement		
Erathem	System	Series	Formation	Symbol									
Cenozoic	Neogene	Quaternary		Q	[Symbol]	200–560							
		Miocene	Pliocene	Kuqa	N ₁ k	[Symbol]	450–3600				1.64	Late Himalayan	
			Kangcun	N ₁ k	[Symbol]	650–1600					5.2	Middle Himalayan	
				Jidike	N ₁ j	[Symbol]	200–1300						
	Paleogene	Oligocene	Suweiyi	E ₁ s	[Symbol]	150–600					23.3	Early Himalayan	
		Eocene/Palcoocene	Kumugeliemu	E ₁ -km	[Symbol]	110–300							
Mesozoic	Cretaceous	Lower	Bashijiqike	K ₁ bs	[Symbol]	100–360					66	Late Yanshanian	
			Baxigai	K ₁ b	[Symbol]	60–490							
			Shushahe	K ₁ s	[Symbol]	140–1100							
			Yageliemu	K ₁ y	[Symbol]	60–250							
	Jurassic	Upper	Kelazha	J ₁ k	[Symbol]	12–60						145	Middle Yanshanian
			Qigu	J ₁ q	[Symbol]	100–350							
		Middle	Qiakemake	J ₁ q	[Symbol]	60–150							
			Kezilenuer	J ₁ kz	[Symbol]	400–800							
	Lower	Yangxia	J ₁ y	[Symbol]	450–600								
		Ahc	J ₁ a	[Symbol]	90–400								
Triassic	Upper	Taliqike	T ₁ t	[Symbol]	200						201	Indosinian	
		Huangshanjie	T ₁ h	[Symbol]	80–850								
	Middle	Kelamayi	T ₁ k	[Symbol]	400–550								

Figure 2. Mesozoic–Cenozoic stratigraphic system in the Dibeï tectonic belt, Kuqa Depression (modified from Xiongqi Pang, 2019 [16] and Xiaowen Guo, 2016 [17]).

The Dibei tight gas field is in the middle of the Yiqiklike thrust belt. Oil, gas, and water all exist at the top of the anticline in this tight gas field, and there is a lot of natural gas in the tight reservoirs on the slope [16,36]. According to the oil and gas exploration results, commercial gas was discovered in the YN2, DX1, DB102, and DB104 wells along the slope, while the YN4 and YS4 far away from the slope have no commercial value. Studies on source rocks indicated that the oil and gas in the J₁a reservoir mainly came from the Jurassic source rocks, and the Middle-Upper Triassic strata also provided some natural gas [37,38].

3. Samples and Methods

In order to study the porosity and permeability and diagenesis characteristics of the reservoir, core samples were collected from PCTO. These samples are relatively uniformly distributed from 8 typical wells, with depths ranging from 4000 to 5100 m.

The CMS-300 automatic porosity and permeability measuring instrument was utilized to determine the porosity and permeability under a confining pressure of about 30 MPa. Scanning electron microscopy (SEM) was used to detect the types of clay minerals in the reservoir to determine the reservoir space type and condition of the clay minerals in the reservoir. QUANTA 200 SEM was used to detect representative samples. A total of 105 samples from 8 wells were analyzed for particle size, diagenetic characteristics, and porosity. The thin section is dyed with blue epoxy resin to mark the reservoir space, and the porosity of the thin section is calculated by the point method.

The DSG600 transparent reflection polarization fluorescence microscope was used to analyze the fluid inclusions of 31 samples from 8 wells in the Dibei gas reservoir to determine the hydrocarbon charging time. Petrographic and micro temperature methods were used to analyze the shape, size, distribution, color, and fluorescence of inclusions. The fluid inclusion was heated from room temperature to 0.5 °C/min until the phase boundary disappeared; the temperature was recorded in the state and maintained at a stationary temperature for 2 min. Then, the temperature of fluid inclusions dropped. When there were some other bubbles, the process was repeated to achieve the same uniform temperature.

By integrating data such as formation thickness, lithology, absolute age, erosion thickness, measured vitrinite reflectance (R_o), and borehole temperature, the burial and temperature history was reconstructed using BasinMod 1D software. In order to reconstruct the evolution of tight sandstone reservoirs and point out the influence of diagenesis, the model from Ruifei Wang, 2011 [39], was used to estimate the influence of different diagenesis on the reservoir. The model links reservoir porosity evolution to diagenetic stages, thereby quantifying the contributions of different diagenesis.

4. Results

4.1. Lithofacies Characteristics

According to the classification scheme of Folk [40] and the results of thin section analysis, the sandstone from the J₁a Formation in the Dibei structural belt is dominated by lithic sandstone and feldspar lithic sandstone (Figure 3). In the lithic sandstone, the relative content of rock fragments is 27.3%~86.4%, with an average of 81.2%; the content of feldspar is 5.65%~62.7%, with an average of 39.4%; the content of quartz is 1.2%~73.6%, with an average of 52.7%. The sorting of sandstone is medium-good, the roundness is mainly sub-angular-sub-round, the compositional maturity of the rock is low, and the structural maturity is medium. The sorting of sandstone is medium-good, the rounding is mainly sub-angular and sub-circular, the compositional maturity of the rock is low, and the structural maturity is medium.

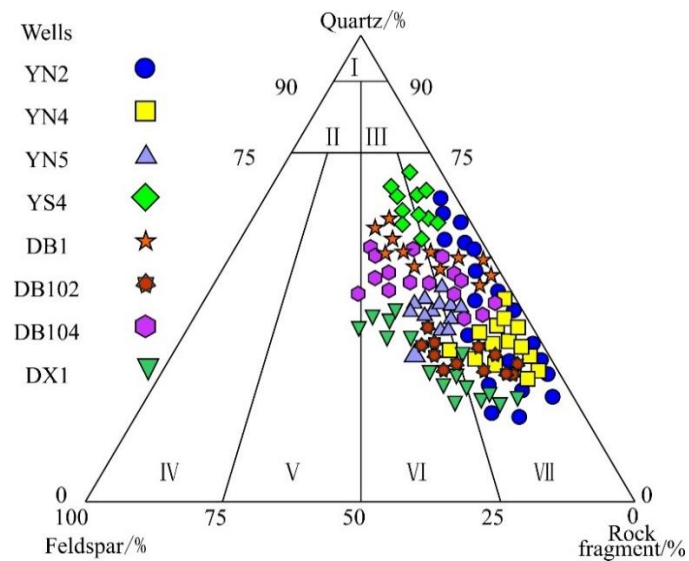


Figure 3. Figure indicating the composition of J_1a tight sandstone from Dibeig gas field, eastern Kuqa Depression (number of samples = 105). Note: I—quartz sandstone; II—feldspar quartz sandstone; III—lithic quartz sandstone; IV—arkose sandstone; V—lithic arkose; VI—feldspar lithic sandstone; VII—lithic sandstone.

4.2. Reservoir's Porosity and Permeability

The relationship between porosity and permeability of 93 sandstone core samples from J_1a sandstone is indicated in Figure 4. The porosity values of the J_1a Formation range from 1% to 12%. The porosity values of most samples are between 2% and 10%, with an average of 9.1%. The range of permeability values is between 0.01 and 86.8 mD, with 85% of the values varying from 0.01 to 1 mD (average 0.09 mD), which has the typical characteristics of tight sandstone gas.

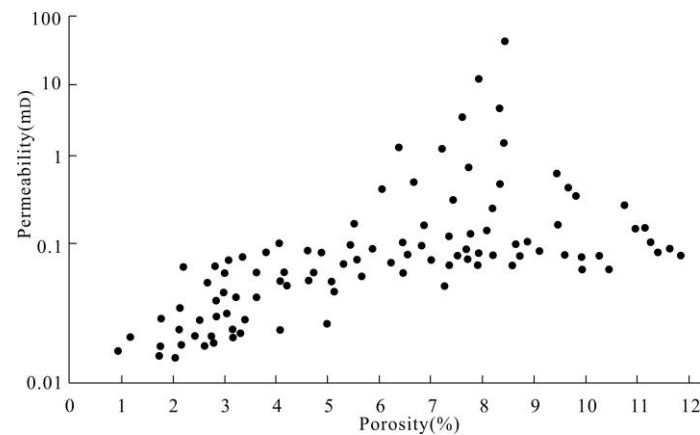


Figure 4. Diagram of the relationship between permeability and porosity.

4.3. Pore Systems

Based on the thin section observation and SEM analysis, there exist three types of storage space, namely primary intergranular pores (Figure 5a), secondary dissolution pores (Figure 5b–d), and fractures (Figure 5e,f). The thin section porosity (by point counting) of the tight reservoir of the J_1a Formation ranges from a trace level (less than 1%) to 9.9% (average 4.4%). The range of primary intergranular porosity is between a trace level and 5.6% (average 1.8%). The skeleton particles are dissolved to form secondary pores, which range from trace to 7.8% (average 3.4%). The J_1a Formation is buried deeply (more than 4000 m), so the original pores are severely damaged; therefore, primary intergranular pores are not the major storage space in the reservoir. The pores formed by dissolution,

namely intergranular dissolution pores (Figure 5b) and intragranular dissolution pores (Figure 5c,d), are the second type of storage space. Because of the high ratio of feldspar and rock cuttings, lots of dissolution pores are generated, providing good storage space for oil and gas. The third type is a fracture (Figure 5e,f), which can be observed in the samples.

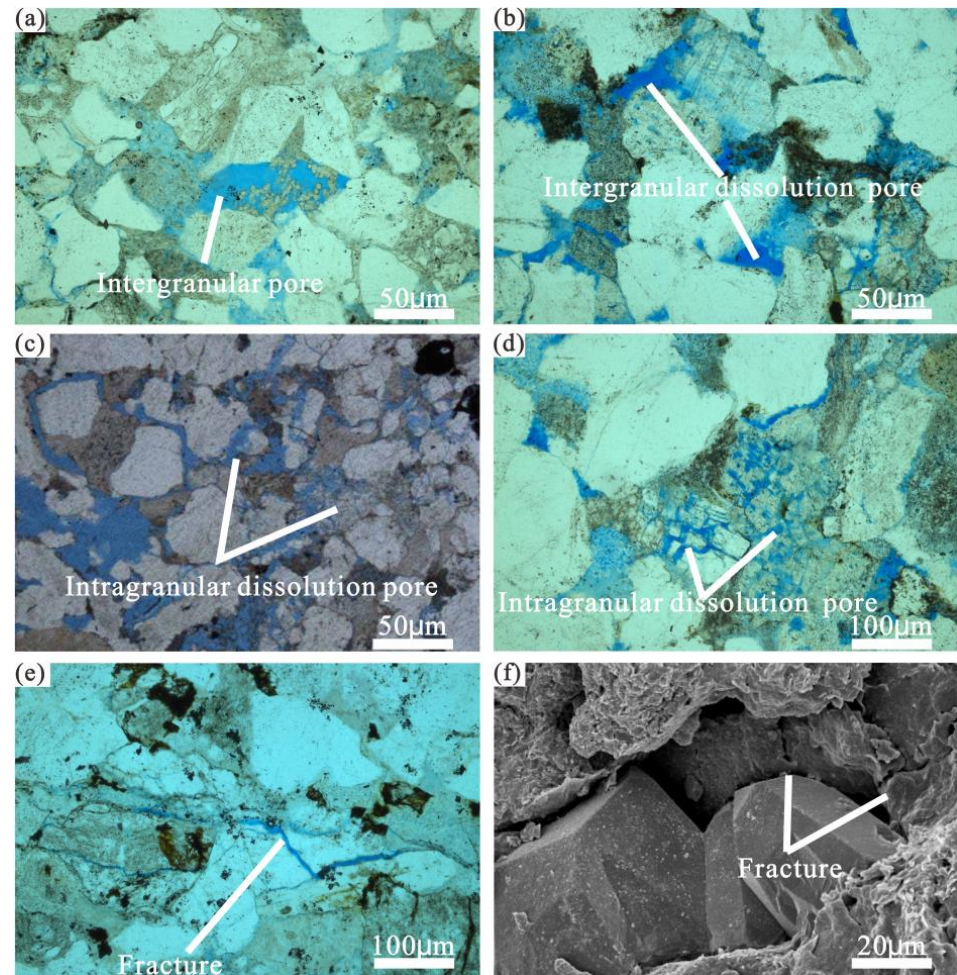


Figure 5. Space type of J₁a sandstone from Dibe area. (a) YN5, 4931.82 m, intergranular pores; (b) YN2, 4845.8 mm, intergranular dissolution pores; (c,d) YN4, 4189.6 m, intragranular dissolution pores; (e,f) DB102, 5056.5 m, fractures.

4.4. Diagenesis Types

4.4.1. Compaction

The main factor causing the decrease in porosity of clastic rocks is compaction [7,41]. The degree of compaction can be determined by the contact relationship of the particles. Compaction significantly reduces the porosity of tight reservoirs in the J₁a Formation. Firstly, the cuttings deform during the compaction process, resulting in point contact, line contact, and suture contact, which fills the intergranular pore and blocks pore throats (Figure 6a,b). Secondly, in the middle diagenetic stage, the acid generated from organic matter dissolved the feldspar debris and led to the weakening of the rock framework, which further compacted the framework particles [42]. Finally, the J₁a Formation is currently buried at a depth of about 4000–5000 m, which results in highly effective stress in the overburden and strong compaction through dissolution.

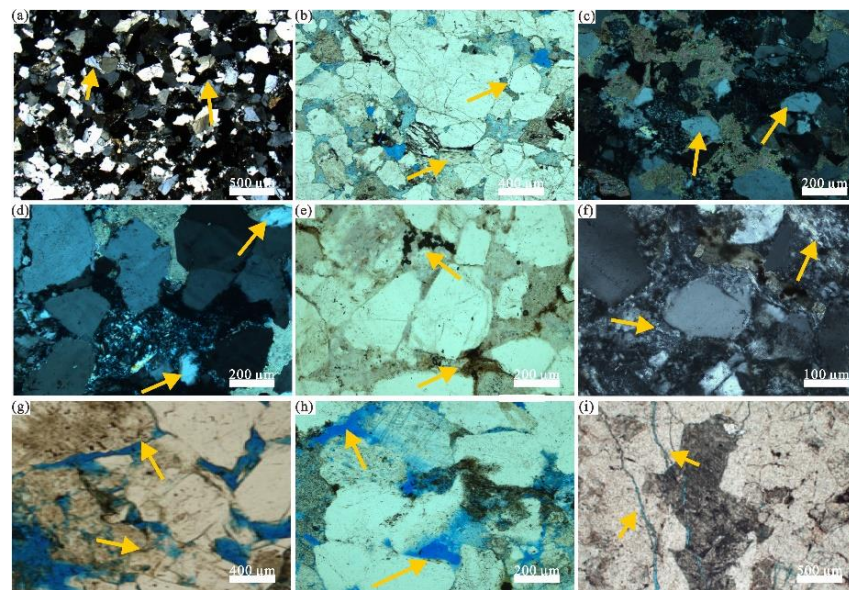


Figure 6. Diagenetic features of the J_{1a} sandstone reservoir. (a) PPL, grain line contact and stylolite contact (Well YN5, 4922.09 m); (b) PPL, grain line contact (Well YN4, 4121.58 m); (c) XPL, calcite cement (Well YN4, 4127.69 m); (d) PPL, calcite cement (Well YN2, 4841.63 m); (e) XPL, quartz overgrowth (Well DX 1, 4854.32 m); (f) PPL, quartz overgrowth (Well DB 102, 5004.39 m); (g) PPL, feldspar overgrowth (Well DX 1, 4858.74 m); (h) PPL, feldspar dissolution (Well YN2, 4839.26 m); (i) PPL, structural fractures (Well YN5, 4839.86 m). PPL—plane-polarized light; XPL—cross-polarized light.

The relationship between total intergranular volume and cement content shows that compaction reduces porosity more than cementation (Figure 7), with three exceptions. The compaction rate is 27.9%~76.8% (average 61.9%), and the cementation rate is 4.3%~62.9% (average 14.3%). According to the porosity evolution model of [39], the porosity loss during compaction is calculated. The average reduction rate of compacted porosity is 62.3%, and the average reduction rate of cemented porosity is 15.2%, which basically corresponds to the result in Figure 7. Comprehensive analysis shows that compaction is the main diagenesis causing porosity damage.

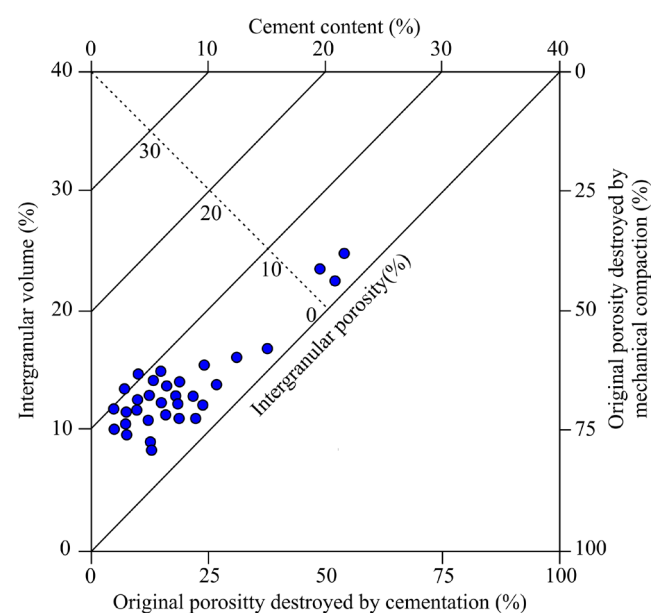


Figure 7. The relationship between the intergranular volume and the cementation volume of the J_{1a} tight reservoir (modified from Longlong Liu, 2020 [43]).

4.4.2. Cementation

Cementation is another major factor affecting the porosity of the reservoir. Calcite is a widely distributed cement in the J₁a unit, and its content is uneven (0–31%, average of 18.6%). Occasionally, calcite blocks of cement were distributed around the detrital grains (Figures 6c and 8a), but calcite cement usually filled the intergranular pores as microcrystalline (Figure 6d), indicating a high degree of carbonate cementation. Although cement can limit compaction, some of the original porosity damaged by compaction is preserved, but in general, the destructive effect of carbonate cement on the reservoir is more apparent.

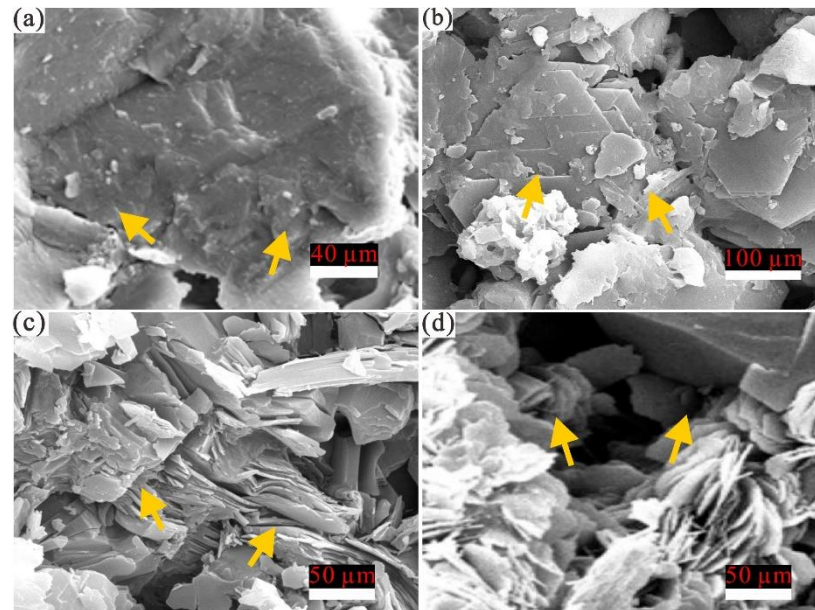


Figure 8. Diagenetic characteristics of the Ahe reservoir shown under the SEM. (a) Calcite cement (Well YN2, 4841.63 m); (b) Kaolinite cement (Well DX1, 4855.45 m); (c) Illite cement (Well YN5, 4930.58 m); (d) Chlorite cement (Well DX1, 4856.85 m).

Silica cementation is a key diagenetic process that causes the deterioration of sandstone reservoir quality. Silica cement is overgrown around single-crystal quartz grains. Quartz overgrowth is distributed on the surface of the quartz particles (Figure 6e,f). The volume content of quartz overgrowth in sandstone ranges from 51% to 79% (average of 67.9%). Feldspar overgrowth was occasionally detected (Figure 6g), which provided material for the corrosion process.

The total content of clay minerals determined by XRD was from 3.9% to 14.5%, with an average of 12.3%. There are three kinds of clay minerals in the sample, and their contents are: kaolinite (10.9%–27.8%, average of 38.6%), illite (7.9%–25.2%, average of 36.3%), and chlorite (8.5%–26.2%, average of 24.6%). Kaolinite is an important clay mineral in the J₁a Formation. The morphology of kaolinite is usually booklet form, and it occupies intragranular and intergranular pores. The kaolinite clay minerals are closely associated with dissolved feldspar crystals, indicating that the kaolinite minerals are formed by the dissolution of unstable feldspar. Moreover, the chemical reaction of feldspar with CO₂ resulted in the formation of kaolinite on the feldspar surface. Kaolinite is usually associated with illite and mixed illite/montmorillonite layers. During the middle diagenetic stage, a large amount of unstable feldspar was dissolved by the meteoric water, which may cause the feldspar to transform into kaolinite. It may be the reason for the low feldspar content [44]. Illite is another important clay mineral found in the J₁a Formation. Illite usually exists in a flake form. At times, illite seems to grow at the expense of kaolinite. However, illite is not fully developed (Figure 8c), probably because the kaolinite that formed illite was not buried deeply. Chlorite is another minor clay mineral in this sandstone. The morphology

of chlorite clay is dominated by pore-filling crystals. Chlorite cladding is at the edge (Figure 8d), which is thought to form during the early diagenetic stage. The intergranular pores are mainly filled with chlorite, accompanied by minerals such as kaolinite and illite.

4.4.3. Dissolution

Dissolution is a critical factor in forming good-quality reservoirs [45,46]. According to the above analysis, compaction and cementation severely damaged the primary pores. However, the dissolution of feldspar and clastic rocks in the later stage formed secondary pores, which are the main pores of the J₁a tight sandstone. The thin section observation results indicate the secondary pores of the J₁a Formation are widely distributed, indicating that dissolution is major diagenesis. Feldspar usually dissolves partially along cleavage planes and fractures, resulting in the formation of numerous secondary intragranular pores (Figure 6h). In the regions with strong dissolution, the secondary intergranular and intragranular pores are widely developed, and the porosity is high. Therefore, the dissolution of feldspar is a decisive factor in the development of secondary pores [47].

It is worth mentioning that the thrust structure in the Dibe area is strong and lateral pressure is obvious, which causes the pores to be reduced [22]. However, structural fractures also make the fractures more developed (Figure 6i).

4.5. Burial History and Fluid Inclusion Characteristics

The burial-thermal evolution history was reconstructed to clarify the diagenetic process and pore evolution, as shown in Figure 9. The burial curve is taken from well DB102. In the Paleogene, the J₁a group began to deposit at a faster rate, and when the J₁a was deposited, the group was uplifted and eroded; Then, the J₁a layer continued to be buried rapidly. At about 4.5 Ma ago, the deposition rate increased significantly; in the early Quaternary, the J₁a Formation was buried at a depth of more than 4000 m.

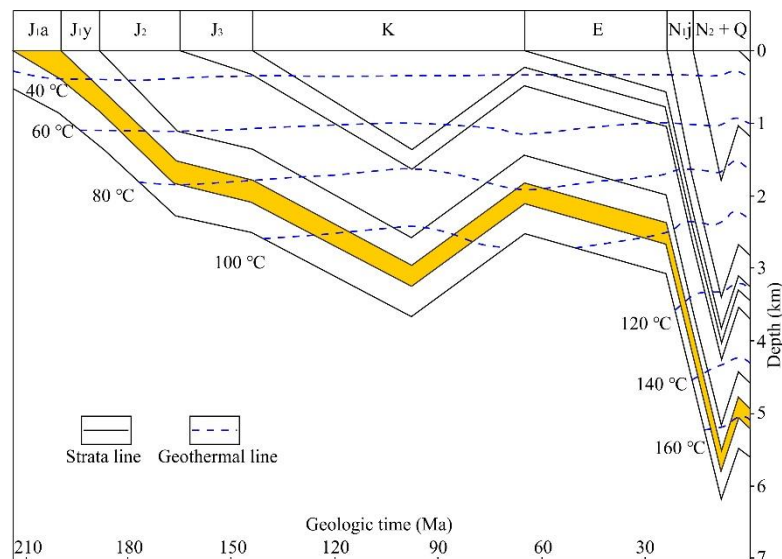


Figure 9. Burial, thermal history, and geothermal line of well DB102.

The fluid inclusion characteristics of the samples are shown in Figure 10. The aqueous inclusions in the same period as the hydrocarbon inclusions exist in wells DB102, YN2, YN4, and YN5. The homogenization temperature of the inclusion has two peaks, indicating the two periods of oil and gas charging. The temperature range of the first peak is 85~110 °C (12 Ma), and the second is 115~140 °C (4.5 Ma) (Figure 10). Under ultraviolet light, the first group of fluid inclusions showed yellow fluorescence (Figure 11a), indicating that the charged hydrocarbons have low maturity. The second group shows blue fluorescence (Figure 11b), suggesting that the charged hydrocarbon was of high maturity.

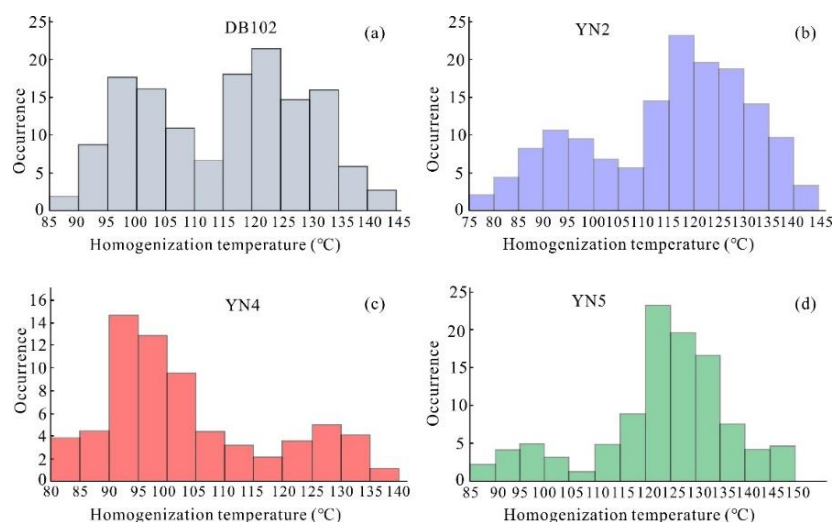


Figure 10. Homogenization temperatures of aqueous inclusions coeval with hydrocarbon inclusions in the Dibe area. (a–d) Homogenization temperatures for DB102 well, YN2 well, YN4 well, and YN5 well, respectively.

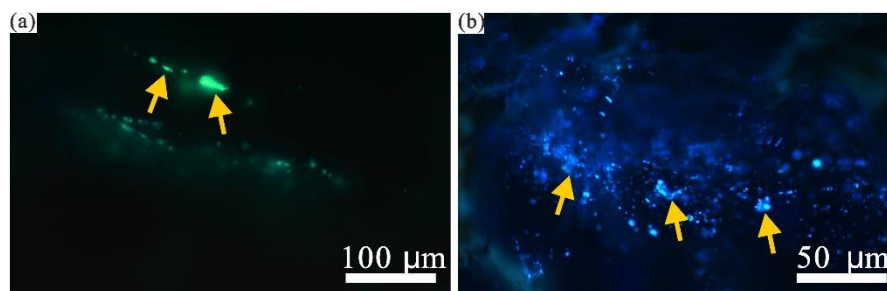


Figure 11. Micrographs of hydrocarbon inclusions in the J_1a Formation under UV light in the Well DB102. (a) Yellow fluorescence; (b) blue-white fluorescence.

5. Discussion

5.1. Diagenetic Evolution

According to the structural relationship [16,33] and diagenetic characteristics, three basic diagenetic stages in the Dibe area have been determined. Based on the standard “Diagenetic Stages of Clastic Rocks” (SY/T5477-2003) from China, the J_1a Formation has experienced three stages: Eodiagenesis, A and B substage of mesogenetic diagenesis. During Eodiagenesis, the paleo-temperature range was from paleo-normal temperature to 85 °C. The pore types were mainly primary pores with a little secondary pore. R_o was usually less than 0.5%; during A substage of mesogenetic diagenesis, the paleotemperature ranged from 85 °C to 14 °C, and the R_o ranges from 0.5% to 1.3%. The organic acid yield was high, and the pore types were mainly secondary pores; during the B substage of mesogenetic diagenesis, the paleotemperature range is 140–175 °C, the R_o range is 1.3–2.0%, and the rocks are densified with fractures. The diagenetic stages and pore evolution are shown in Figure 12.

Eodiagenesis: The first stage: the sandstone of the J_1a Formation has undergone long-term shallow burial and late rapid deep burial. It is the Eodiagenesis stage dominated by compaction, with the development of siliceous cement and kaolinite; **A substage of mesogenetic diagenesis:** this stage is the Paleocene–late Pliocene, low-maturity organic matter produces organic acid, and secondary pores are formed in soluble minerals such as dissolved feldspar and rock fragments. The third stage is the B sub-stage of Mesozoic diagenesis from Late Neogene to Quaternary, with high maturity of organic matter [22]. The content of organic acid decreases, the carbonate cementation increases in the late stage, and

the reservoir quality continues to deteriorate [16]. Under the strong tectonic compression, the compaction is further strengthened, and the porosity is further reduced [22].

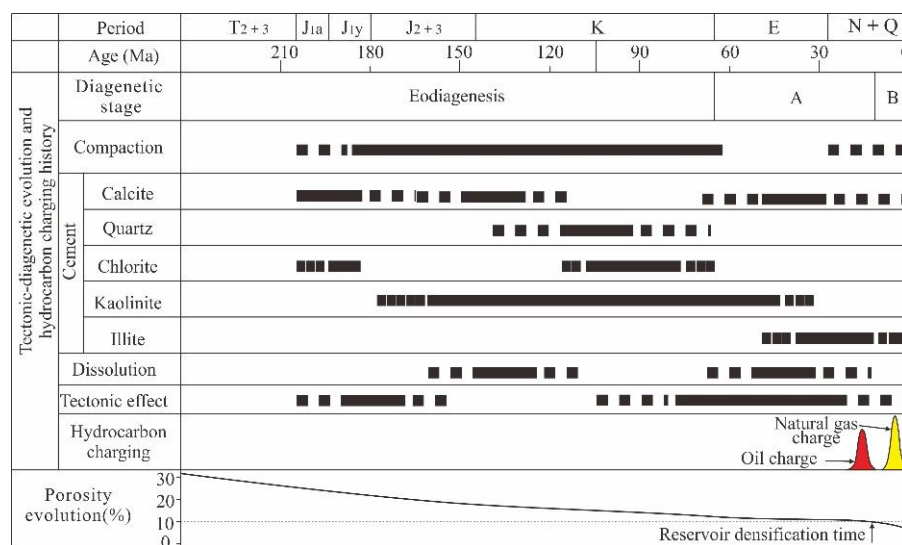


Figure 12. Diagenesis and porosity evolution of the J₁a Formation. A is A substage of mesogenetic diagenesis; B is B substage of mesogenetic diagenesis.

5.2. Controlling Factors of Tight Sandstone

5.2.1. Diagenesis

Destructive Diagenesis

According to Figure 8, the compaction rate is 27.9%~76.8% (average 61.9%). Therefore, compaction is considered to be the main diagenetic process causing porosity deterioration.

Cementation affects reservoir quality [48–50]. However, the cementation is not obvious based on the result calculated by [39] (the average cementation rate is 15.2%). In addition, the compaction rate of samples with a high cementation rate is low, indicating that early strong cementation inhibited mechanical compaction (Figure 7). The reason is that carbonate cement is formed by the formation of water with high ion content, and these types of cement fill the space between particles. With the increase in burial, the types of clay minerals change greatly, affecting the reservoir quality [51]. Moreover, because of the enrichment of alkaline and K⁺ by dissolution, kaolinite is transformed into illite, further reducing the physical properties of the rock, but the depth of illite is not low enough, so illite cement has not been well developed.

Constructive Diagenesis

Although the compaction degree of sandstone is strong, good-quality reservoirs still exist in some areas. The research shows that the secondary dissolution porosity is the main storage space (average thin section porosity is 3.1%), so good-quality tight sandstone reservoirs are mainly affected by dissolution. To evaluate the dissolution effect, the diagram between sheet porosity and feldspar content is drawn. Feldspar is conducive to the occurrence of dissolution, resulting in the generation of secondary dissolution pores (Figure 13). Based on the model from Ruifei Wang, 2011 [39], the dissolution of feldspar and rock fragments increases the porosity by about 10%. Therefore, for high-quality tight sandstone, dissolution is the most important diagenetic process. In addition, the enrichment of kaolinite is also an important part of a high-quality reservoir. The enrichment of kaolinite is also evidence of the strong dissolution of feldspar because the dissolution of feldspar is associated with kaolinite [52].

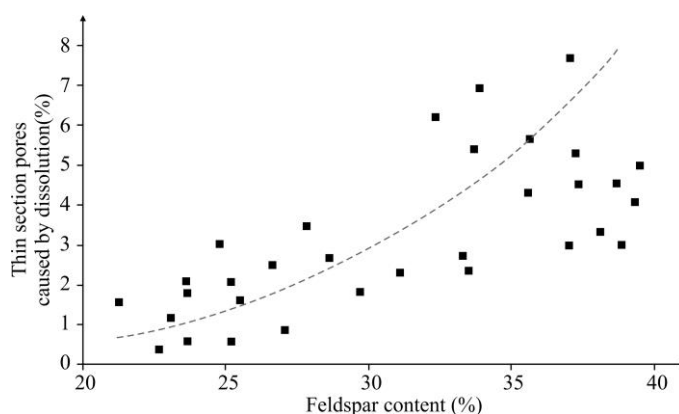


Figure 13. Secondary dissolution pores versus feldspar content.

Tectonism Has Both Destructive and Constructive Effects

Tectonism mostly carries out the secondary transformation of tight reservoirs. This transformation has both advantages and disadvantages for reservoir physical properties, and the overall advantages outweigh the disadvantages. Specifically, in the study area, on the one hand, structural compression leads to further compaction of the reservoir, resulting in the decrease in porosity [53], which has an adverse impact on the physical properties of the reservoir. On the other hand, tectonism will cause the formation of structural fractures in tight reservoirs [54]. Some structural fractures will be further dissolved and expanded under the action of organic acid to form structural dissolution fractures and become a good reservoir space. Some reticular and extended fractures will communicate with isolated residual pores, which greatly improves the permeability of reservoir. Statistics of some core data and cast thin section analysis data [16] show that under the same conditions, the average porosity and permeability values of the reservoir with fracture development are obviously higher than those of the reservoir without fracture development (Table 1). Fractures can effectively improve the porosity and permeability of tight reservoirs. The fracture development area formed by tectonic movement is often a favorable position to form tight sandstone reservoirs. This is consistent with the research results of the literature [2,12].

Table 1. Porosity and permeability of the J₁a sandstone in Dibe area (part of the data is from Hailiang Kang [24]).

Wells	Measured Porosity/%						Measured Permeability/mD					
	Samples with Developed Fractures			Samples without Developed Fractures			Samples with Developed Fractures			Samples without Developed Fractures		
	Min	Max	Ave	Min	Max	Ave	Min	Max	Ave	Min	Max	Ave
YN4	1.19	13.18	9.21	0.89	12.97	7.39	0.038	3160	97.6	0.006	63	1.936
YS4	3.26	12.35	8.73	1.63	16.21	8.36	0.09	926	81.2	0.009	89	1.942
YN2	2.63	13.96	5.62	0.28	15.86	5.48	0.349	392	36.4	0.013	52	1.09
YN5	2.36	9.18	5.65	0.69	12.63	5.91	0.98	2659	258.8	0.021	476	5.27
Ave		8.23			6.95			128.37			2.54	

Note: Min = Minimum; Max = Maximum; Ave = Average.

5.2.2. Oil and Gas Charge and Overpressure

The water in the reservoir can be displaced by charged oil and gas, thereby altering the environment and inhibiting late cementation [55]. Inclusions contain information on the hydrocarbon generation and accumulation, so fluid inclusion is a feasible index to determine the oil and gas charging time [56,57]. The homogenization temperature of fluid inclusions shows that hydrocarbon charging can be divided into two stages at 12 Ma and 4.5 Ma. Late cementation did not form during hydrocarbon charging (Figure 13); therefore, hydrocarbon

charging inhibits the formation of late carbonate types of cement, which can also serve as evidence for the lack of late carbonate types of cement. In addition, the overpressure preserves the primary pores well and enables favorable conditions for dissolution [58,59]. The overpressure in the Dibei structural belt originates from hydrocarbon generation [60]. According to the above analysis, the Upper Triassic and Middle-Lower Jurassic source rocks are dominant in the Kuqa depression. With the evolution of source rocks, overpressure originating from hydrocarbon generation is transferred to nearby reservoirs, resulting in abnormal reservoir pressure [61]. The source rocks of the Triassic and Jurassic reached the hydrocarbon generation peak and formed overpressure at 23–12 Ma. In this stage, the sandstone reservoir was not densified (porosity greater than 10%) (Figure 9); the pressure coefficient of the Dibei structural belt generally exceeds 1.7, and the pressure coefficient in some areas exceeds 1.8 [61]. Therefore, the occurrence of overpressure is conducive to preserving the primary pores.

5.3. Sweet Spot Prediction

The geological characteristics of the Dibei gas reservoir are as follows: the faults formed by the tectonic movement in Yanshanian and Himalayan periods connect the source rocks and reservoirs, as well as the source rocks and caprocks, forming an oil and gas transportation system [54]. Because it is close to the center of Yangxia sag and the distance between hydrocarbon and reservoir is close, natural gas has obvious vertical, lateral, and near-source migration paths [16]; there exist two periods of hydrocarbon charging, namely, early oil charging and late gas charging.

A uniform gas water interface does not exist, and the gas reservoir formed at the high part of the structure is damaged by water and becomes a water layer (Figure 14); reservoir densification is earlier than natural gas charging. The reservoir forming mode of the Dibei gas reservoir is: crude oil filling in the Late Neogene (12 Ma); in the late sedimentary period of Kangcun Formation, the reservoir gradually densified (7 Ma); mature natural gas filling in the early deposition of Kuqa Formation (4.5 Ma), and gas reservoir formed after transformation and adjustment in the Quaternary period (2 Ma). The result basically corresponds to the previous conclusion [22].

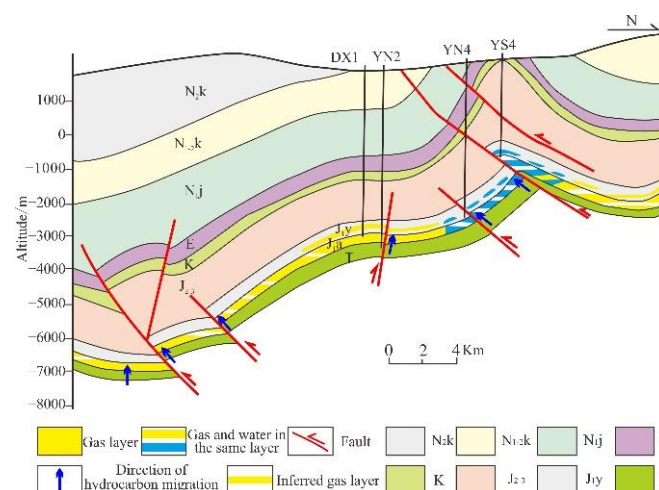


Figure 14. Comprehensive reservoir formation pattern in Dibei area (modified from Xiongqi Pang, 2019 [16] and Song Guo, 2018 [22]).

Based on the previous studies, the natural gas of the J_1a Formation mainly comes from the mixture of Jurassic and Triassic, and mainly from Jurassic [37,38]. Moreover, source rocks can provide a sufficient source for oil and gas accumulation [22].

Fractures can not only serve as good seepage channels but also improve the reservoir space of tight sandstone reservoirs [62,63]. The reservoir of the J_1a Formation in Dibei section of the Kuqa depression is tighter than most tight reservoirs (porosity < 14%,

permeability < 0.1 mD) that produce gas in America [16], but the permeability of section with many fractures is generally high. Through the quantitative relationship between the gas production of drilled wells and the degree of fracture development, it can be found that there is a positive relationship between the degree of fracture development and tight gas production [64]; that is, the higher the degree of fracture development, the higher the tight gas production.

Fracture development areas are mainly distributed at the edge of the Dibei structural belt (Figure 15), while relatively few are in the middle [24,65]. Different from conventional reservoir forming conditions, tight sandstone gas reservoirs are less affected by faults and caprocks [16,22]. Diagenesis is widely developed in this area, which is consistent with the research result of previous scholars [66]. The results of this study and previous studies indicate that dissolution is well developed in the Dibei tectonic belt [24]. Coupling the effective gas intensity of source rock, the fracture development area of the J₁a Formation reservoir, and the favorable area of diagenesis, it is predicted that the sweet spot of tight gas of J₁a Formation in the Dibei area is in the southeast of YN 2 well (Figure 15).

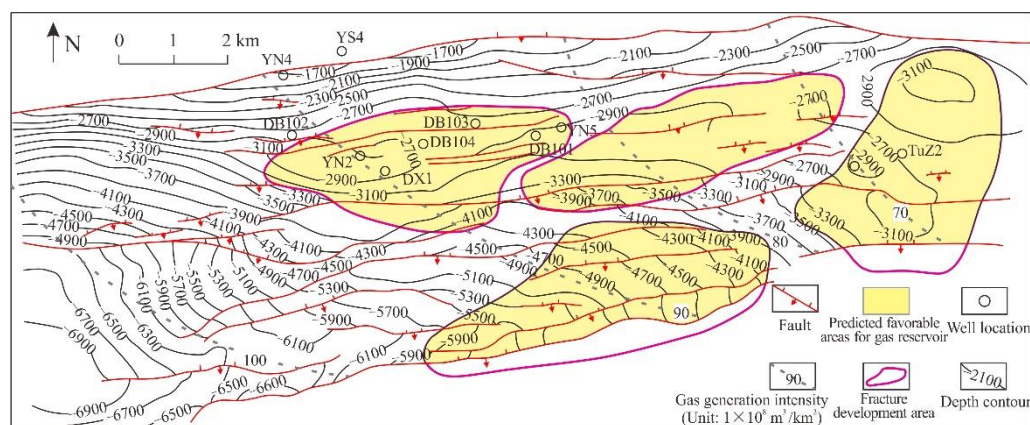


Figure 15. Sweet spots area for J₁a tight sandstone in the Dibei reservoir (the source rock data are from Caineng Zou, 2011 [37]; fracture data are modified from Hailiang Kang, 2016 [24]).

6. Conclusions

This study aimed to reveal the accumulation model of the Dibei gas reservoir in the Kuqa depression and predict the sweet spot area. By comprehensively using petrology, SEM, thermal burial history simulation, and fluid inclusion analysis, the reservoir physical properties, diagenesis, and accumulation mode of tight sandstone gas reservoirs were studied. This study provides a reference for the exploration and development of other areas in the Kuqa depression. The main conclusions are as follows: The tight sandstone of J₁a Formation in the Dibei gas field of Kuqa depression is mainly lithic arkose and feldspathic lithic sandstone, with moderate composition and moderate structural maturity. Secondary dissolution pores are a major part of the pore system. Four important diagenesis processes are determined. Compaction is the main diagenesis that causes porosity reduction, and the contact of suture particles is linear and evenly distributed. The types of cement mainly include carbonate, quartz, and clay cement. The main mineral for dissolution in the J₁a tight sandstone is feldspar. The tectonic movement has constructive and destructive effects on diagenetic evolution. Controlling factors to form good-quality tight sandstone include dissolution and overpressure, and dissolution is dominant. Based on the analysis of diagenetic evolution and reservoir controlling factors, the accumulation mode of the Dibei tight gas reservoir is proposed, and the sweet spot prediction is made according to the accumulation mode. The gas generation intensity of Jurassic source rocks, the fracture development area of the J₁a formation reservoir, and dissolution are the main factors controlling the distribution of sweet spots. It is pointed out that the sweet spot is mainly on the southeast edge of the Dibei gas reservoir. This model and sweet spot prediction

method can be used for the exploration and deployment of other gas reservoirs in the Kuqa depression.

Author Contributions: Conceptualization, G.Z. and X.L.; methodology, M.L.; software, J.Z.; validation, M.L.; resources, C.D.; data curation, J.Z.; writing—original draft preparation, G.Z.; writing—review and editing, D.C.; funding acquisition, X.L. All authors have read and agreed to the published version of the manuscript.

Funding: This research was funded by the National Science and Technology Major Project of China (No. 2016ZX05007–003), Science and Technology Projects of PetroChina (No. T11083), the National Natural Science Foundation of China (No. U1810201), and the Fundamental Research Funds for the Central Universities (Nos. 2020YJSM02, 2021YJSM09).

Institutional Review Board Statement: Not applicable.

Informed Consent Statement: Not applicable.

Data Availability Statement: Not applicable.

Acknowledgments: We are indebted to Zhongyao Xiao (Tarim Oilfield Company, PetroChina) for his insightful suggestions and help in the manuscript.

Conflicts of Interest: The authors declare no conflict of interest.

References

- Dai, J.; Ni, Y.; Qin, S.; Huang, S.; Peng, W.; Han, W. Geochemical characteristics of ultra-deep natural gas in the Sichuan Basin, SW China. *Pet. Explor. Dev.* **2018**, *45*, 619–628. [\[CrossRef\]](#)
- Shanley, K.W.; Cluff, R.M.; Robinson, J.W.; Lantana, K.W.S. Factors controlling prolific gas production from low-permeability sandstone reservoirs: Implications for resource assessment, prospect development, and risk analysis. *AAPG Bull.* **2004**, *8*, 1083–1121. [\[CrossRef\]](#)
- Law, B.E.; Curtis, J.B. Introduction to unconventional petroleum systems. *AAPG Bull.* **2002**, *86*, 1851–1852.
- Alqubalee, A.; Abdullatif, A.; Babalola, L. Characteristics of Paleozoic tight gas sandstone reservoir: Integration of lithofacies, paleoenvironments, and spectral gamma-ray analyses, Rub' al Khali Basin, Saudi Arabia. *Arab. J. Geosci.* **2019**, *12*, 182742801. [\[CrossRef\]](#)
- Zou, C.; Zhu, R.; Liu, K.; Ling, K.; Su, L.; Bai, B. Tight gas sandstone reservoirs in China: Characteristics and recognition criteria-ScienceDirect. *J. Pet. Sci. Eng.* **2012**, *88–89*, 82–91. [\[CrossRef\]](#)
- Wüstefeld, P.; Hilse, U.; Lüders, V. Kilometer-scale fault-related thermal anomalies in tight gas sandstones. *Mar. Pet. Geol.* **2017**, *86*, 288–303. [\[CrossRef\]](#)
- Stroker, T.M.; Harris, N.B.; Elliott, W. Diagenesis of a tight gas sand reservoir: Upper Cretaceous Mesaverde Group, Piceance Basin, Colorado. *Mar. Pet. Geol.* **2013**, *88–89*, 48–68. [\[CrossRef\]](#)
- Chalmers, G.; Bustin, R.M. Geological evaluation of Halfway–Doig–Montney hybrid gas shale–tight gas reservoir, northeastern British Columbia. *Mar. Pet. Geol.* **2012**, *38*, 53–72. [\[CrossRef\]](#)
- U.S. Energy Information Administration. Gas resources in Russia's tight sedimentary basins and their future commercial development. *Gas Ind. Rus.* **2012**, *4*, 34–38.
- Guo, X.B.; Huang, Z.L.; Zhao, L.B.; Han, W.; Ding, C.; Sun, X.W.; Yan, R.T.; Zhang, T.H.; Yang, X.J.; Wang, R.M. Pore structure and multi-fractal analysis of tight sandstone using MIP, NMR and NMRC methods: A case study from the Kuqa depression, China. *J. Pet. Sci. Eng.* **2019**, *178*, 544–558. [\[CrossRef\]](#)
- Huyan, Y.Y.; Pang, X.Q.; Jiang, F.J.; Li, L.L.; Zheng, D.Y.; Shao, X.H. Coupling relationship between tight sandstone reservoir and gas charging: An example from lower Permian Taiyuan Formation in Kangning field, northeastern Ordos Basin, China. *Mar. Pet. Geol.* **2019**, *105*, 238–250. [\[CrossRef\]](#)
- Wang, E.; Wang, Z.; Pang, X.; Zhang, Z.; Wang, Z.M.; Wu, Z.; Liang, Y.; Feng, Y.; Zhang, Z. Key factors controlling hydrocarbon enrichment in a deep petroleum system in a terrestrial rift basin—A case study of the uppermost member of the upper Paleogene Shahejie Formation, Nanpu Sag, Bohai Bay Basin, NE China. *Mar. Pet. Geol.* **2019**, *107*, 572–590. [\[CrossRef\]](#)
- Zheng, D.Y.; Pang, X.Q.; Ma, X.H.; Li, C.R.; Zheng, T.Y.; Zhou, L.M. Hydrocarbon generation and expulsion characteristics of the source rocks in the third member of the Upper Triassic Xujiahe Formation and its effect on conventional and unconventional hydrocarbon resource potential in the Sichuan Basin. *Mar. Pet. Geol.* **2019**, *109*, 175–192. [\[CrossRef\]](#)
- Xu, Z.; Jiang, S.; Liu, L.; Wu, K.; Li, R.; Liu, Z. Natural gas accumulation processes of tight sandstone reservoirs in deep formations of Songliao Basin, NE China. *J. Nat. Gas Sci. Eng.* **2020**, *83*, 103610. [\[CrossRef\]](#)
- Chen, Q.; Deng, Y.; Wei, J.; Ma, G.; Long, L.; Xiao, W.; Li, W.; Zhang, L. Types, distribution and play targets of Lower Cretaceous tight oil in Jiuquan Basin, NW China. *Pet. Explor. Dev.* **2018**, *45*, 212–222. [\[CrossRef\]](#)

16. Pang, X.Q.; Peng, J.W.; Jiang, Z.X.; Yang, H.J.; Wang, P.W.; Jiang, F.J.; Wang, K. Hydrocarbon accumulation processes and mechanisms in Lower Jurassic tight sandstone reservoirs in the Kuqa subbasin, Tarim Basin, northwest China: A case study of the Dibeitight gas field. *Am. Assoc. Pet. Geol. Bull.* **2019**, *103*, 769–796. [[CrossRef](#)]
17. Guo, X.; Liu, K.; Jia, C.; Song, Y. Hydrocarbon accumulation processes in the Dabeitight-gas reservoirs, Kuqa Subbasin, Tarim Basin, northwest China. *Am. Assoc. Pet. Geol. Bull.* **2016**, *10*, 1501–1521. [[CrossRef](#)]
18. Lai, J.; Fan, X.; Pang, X.; Zhang, X.; Xiao, C.; Zhao, X.; Han, C.; Wang, G.; Qin, Z. Correlating diagenetic facies with well logs (conventional and image) in sandstones: The Eocene–Oligocene Suweiyi Formation in Dina 2 Gasfield, Kuqa depression of China. *J. Pet. Sci. Eng.* **2019**, *174*, 617–636. [[CrossRef](#)]
19. Sun, S.; Hou, G.T.; Zheng, C.F. Prediction of tensile fractures in KS2 trap, Kuqa depression, NW China. *Mar. Pet. Geol.* **2019**, *101*, 108–116. [[CrossRef](#)]
20. Lu, H.; Lu, X.; Fan, J.; Wang, X.; Fu, X.; Wei, H.; Zhang, B. The controlling effects of fractures on gas accumulation and production in tight sandstone: -a case of jurassic Dibeitight gas reservoir in the east Kuqa foreland basin. *J. Nat. Gas Geosci.* **2015**, *26*, 1047–1056.
21. Shi, C.; Li, Y.; Yuan, W.; Jiang, J.; Xie, Y.; Zhang, R.; Zhou, S. Characteristics on reservoir architecture and quality of tight sandstone reservoirs: Taking Jurassic Ahe formation in Dibeitight area of Kuga foreland basin as an example. *J. China Univ. Min. Technol.* **2021**, *50*, 877–892.
22. Guo, S.; Lyu, X.X.; Zhang, Y. Relationship between tight sandstone reservoir formation and hydrocarbon charging: A case study of a Jurassic reservoir in the eastern Kuqa depression, Tarim Basin, NW China. *J. Nat. Gas Sci. Eng.* **2018**, *52*, 304–316. [[CrossRef](#)]
23. Ju, W.; Wang, K.; Hou, G.; Sun, W.; Yu, X. Prediction of natural fractures in the Lower Jurassic Ahe Formation of the Dibeitight Gasfield, Kuqa depression, Tarim Basin, NW China. *Geosci. J.* **2018**, *22*, 241–252. [[CrossRef](#)]
24. Kang, H.; Lin, C.; Li, H.; Wang, K. Reservoir characteristics and favorable zone prediction of tight sandstone gas of the Ahe Formation in Yinan area Kuqa depression. *Pet. Geol. Exp.* **2016**, *38*, 162–169.
25. Ajdukiewicz, J.M.; Nicholson, P.H.; Esch, W.L. Prediction of deep reservoir quality using early diagenetic process models in the jurassic norphlet formation, Gulf of Mexico. *AAPG Bull.* **2010**, *94*, 1189–1227. [[CrossRef](#)]
26. Lai, J.; Wang, G.; Chai, Y.; Ran, Y.; Zhang, X. Depositional and diagenetic controls on pore structure of tight gas sandstone reservoirs: Evidence from lower Cretaceous Bashijiqike formation in Kelasu thrust belts, Kuqa Depression in Tarim Basin of West China. *Resour. Geol.* **2015**, *65*, 55–75. [[CrossRef](#)]
27. Okunuwajde, S.E.; Bowden, S.A.; Macdonald, D.I.M. Diagenesis and reservoir quality in high-resolution sandstone sequences: An example from the Middle Jurassic Ravenscar sandstones, Yorkshire CoastUK. *Mar. Pet. Geol.* **2020**, *118*, 104426. [[CrossRef](#)]
28. Rafaela, M.; Michael, S.; Turrero, M.J. Diagenetic processes influencing porosity in sandstones from the Triassic Buntsandstein of the Iberian Range, Spain. *Sediment. Geol.* **1996**, *105*, 203–219.
29. Su, N.; Song, F.; Qiu, L.; Zhang, W. Diagenetic evolution and densification mechanism of the Upper Paleozoic tight sandstones in the Ordos Basin, Northern China. *J. Asian Earth Sci.* **2021**, *205*, 104613. [[CrossRef](#)]
30. Du, Z.L.; Wang, F.Y.; Zhang, S.C.; Zhang, B.M.; Liang, D.G. Gas generation history of Mesozoic hydrocarbon kitchen in Kuqa depression, Tarim basin. *Geochimica* **2006**, *35*, 419–431.
31. Zhao, W.; Zhang, S.; Wang, F.; Cramer, B.; Chen, J.; Sun, Y.; Zhang, B.; Zhao, M. Gas systems in the Kuche Depression of the Tarim Basin: Source rock distributions, generation kinetics and gas accumulation history. *Org. Geochem.* **2005**, *36*, 1583–1601. [[CrossRef](#)]
32. Liang, D.G.; Zhang, S.C.; Chen, J.P.; Wang, F.Y.; Wang, P.R. Organic geochemistry of oil and gas in the Kuqa depression, Tarim Basin, NW China. *Org. Geochem.* **2003**, *34*, 873–888. [[CrossRef](#)]
33. Shen, Y.Q.; Lü, X.X.; Guo, S.; Song, X.; Zhao, J. Effective evaluation of gas migration in deep and ultra-deep tight sandstone reservoirs of Keshen structural belt, Kuqa depression. *J. Nat. Gas Sci. Eng.* **2017**, *46*, 119–131. [[CrossRef](#)]
34. Jia, C.Z. *Characteristics of Mesozoic and Cenozoic Structures and Petroleum Occurrence in the Tarim Basin*; Petroleum Industry Press: Beijing, China, 2004.
35. Jia, C.Z.; Li, Q.M. Petroleum geology of Kela-2, the most productive gas field in China. *Mar. Pet. Geol.* **2008**, *25*, 335–343.
36. Pang, X.Q.; Jiang, Z.X.; Jiang, F.J.; Huang, H.D.; Chen, D.X. Formation mechanisms, distribution models, and prediction of superimposed, continuous hydrocarbon reservoirs. *Acta Pet. Sin.* **2014**, *35*, 795–828.
37. Zou, C.N.; Jia, J.H.; Tao, S.Z.; Tao, X.W. Analysis of Reservoir Forming Conditions and Prediction of Continuous Tight Gas Reservoirs for the Deep Jurassic in the Eastern Kuqa Depression, Tarim Basin. *Acta Geol. Sin.* **2011**, *85*, 1173–1186. [[CrossRef](#)]
38. Zhao, M.J.; Zhang, B.M. Source rock conditions for the formation of large gas field in Kuqa foreland depression. *Chin. J. Geol.* **2002**, *37*, 35–44.
39. Wang, R.; Shen, P.; Zhao, L. Diagenesis of deep sandstone reservoirs and a quantitative model of porosity evolution: Taking the third member of Shahejie Formation in the Wendong Oilfield, Dongpu Sag, as an example. *Pet. Explor. Dev.* **2011**, *38*, 552–559. [[CrossRef](#)]
40. Folk, R.L. *Petrology of Sedimentary Rocks*; Hemphill Publishing: Austin, TX, USA, 1980.
41. Rezaee, R.; Saeedi, A.; Clennell, B. Tight gas sands permeability estimation from mercury injection capillary pressure and nuclear magnetic resonance data. *J. Pet. Sci. Eng.* **2012**, *88–89*, 92–99. [[CrossRef](#)]
42. Bjørlykke, K.; Høeg, K. Effects of burial diagenesis on stresses, compaction and fluid flow in sedimentary basins. *Mar. Pet. Geol.* **1997**, *14*, 267–276. [[CrossRef](#)]
43. Liu, L.; Li, Y.; Dong, H.; Sun, Z. Diagenesis and reservoir quality of Paleocene tight sandstones, Lishui Sag, East China Sea Shelf Basin. *J. Pet. Sci. Eng.* **2020**, *195*, 107615. [[CrossRef](#)]

44. Bjørlykke, K.; Jahren, J. *Sandstones and Sandstone Reservoirs. Petroleum Geoscience: From Sedimentary Environments to Rock Physics*, 2nd ed.; Springer: Berlin/Heidelberg, Germany, 2015.
45. Dou, W.; Liu, L.; Wu, K.; Xu, Z.; Feng, X. Origin and significance of secondary porosity: A case study of upper Triassic tight sandstones of Yanchang Formation in Ordos basin, China. *J. Pet. Sci. Eng.* **2017**, *149*, 485–496. [[CrossRef](#)]
46. Zhang, Y.; Tian, J.; Zhang, X.; Li, J.; Liang, Q.; Zheng, X. Diagenesis Evolution and Pore Types in Tight Sandstone of Shanxi Formation Reservoir in Hangjinqi Area, Ordos Basin, Northern China. *Energies* **2022**, *15*, 470. [[CrossRef](#)]
47. Higgs, K.E.; Zwingmann, H.; Reyes, A.G.; Funnell, R.H. Diagenesis, porosity evolution, and petroleum emplacement in tight gas reservoirs, Taranaki Basin, New Zealand. *J. Sediment. Res.* **2007**, *77*, 1003–1025. [[CrossRef](#)]
48. Oluwadebi, A.G.; Taylor, K.G.; Dowe, P.J. Diagenetic controls on the reservoir quality of the tight gas Collyhurst Sandstone Formation, Lower Permian, East Irish Sea Basin, United Kingdom. *Sediment. Geol.* **2018**, *371*, 55–74. [[CrossRef](#)]
49. Busch, B.; Becker, I.; Koehrer, B.; Adelman, D.; Hilgers, C. Porosity evolution of two Upper Carboniferous tight-gas-fluvial sandstone reservoirs: Impact of fractures and total cement volumes on reservoir quality. *Mar. Pet. Geol.* **2019**, *100*, 376–390. [[CrossRef](#)]
50. Wu, H.; Zhao, J.; Wu, W.; Li, J.; Huang, Y.; Chen, M. Formation and diagenetic characteristics of tight sandstones in closed to semi-closed systems: Typical example from the Permian Sulige gas field. *J. Pet. Sci. Eng.* **2021**, *199*, 108248. [[CrossRef](#)]
51. Luo, L.; Meng, W.; Gluyas, J.; Tan, X.; Gao, X.; Feng, M.; Kong, X.; Shao, H. Diagenetic characteristics, evolution, controlling factors of diagenetic system and their impacts on reservoir quality in tight deltaic sandstones: Typical example from the Xujiahe Formation in Western Sichuan Foreland Basin, SW China. *Mar. Pet. Geol.* **2019**, *103*, 231–254. [[CrossRef](#)]
52. Sun, D.; Liu, X.; Li, W.; Lu, S.; He, T.; Zhu, P.; Zhao, H. Quantitative evaluation the physical properties evolution of sandstone reservoirs constrained by burial and thermal evolution reconstruction: A case study from the Lower Cretaceous Baxigai Formation of the western Yingmaili Area in the Tabei Uplift, Tarim. *J. Pet. Sci. Eng.* **2022**, *208*, 109460. [[CrossRef](#)]
53. Zhang, N.; Liu, L.; Su, T.; Dai, Q.; Zhao, Y. Reservoir characteristics and main controlling factors of the lower Jurassic tight sandstone in eastern Kuga Depression. *Acta Sedimentol. Sin.* **2015**, *33*, 160–169.
54. Liu, G.; Zeng, L.; Zhu, R.; Gong, L.; Ostadhassan, M.; Mao, Z. Effective fractures and their contribution to the reservoirs in deep tight sandstones in the Kuqa Depression, Tarim Basin, China. *Mar. Pet. Geol.* **2020**, *124*, 104824. [[CrossRef](#)]
55. Yuan, D.; Zhang, Z.; Liu, H. Effect of hydrocarbon charging on cementation of late carbonate minerals. *J. Oil Gas Technol.* **2005**, *27*, 298–300.
56. Tobin, R.C.; McClain, T.; Lieber, R.B.; Ozkan, A.; Banfield, L.A.; Marchand, A.M.E.; McRae, L.E. Reservoir quality modeling of tight-gas sands in Wamsutter field: Integration of diagenesis, petroleum systems, and production data. *Am. Assoc. Pet. Geol. Bull.* **2010**, *94*, 1229–1266. [[CrossRef](#)]
57. Xu, Z.; Liu, L.; Wang, T.; Gao, X.; Dou, W.; Xiao, F.; Zhang, N.; Song, X.; Ji, H.; Xu, Z.; et al. Application of fluid inclusions to the charging process of the lacustrine tight oil reservoir in the Triassic Yanchang Formation in the Ordos Basin, China. *J. Pet. Sci. Eng.* **2017**, *149*, 40–55. [[CrossRef](#)]
58. Duan, W.; Li, C.F.; Luo, C.; Chen, X.G.; Bao, X. Effect of formation overpressure on the reservoir diagenesis and its petroleum geological significance for the DF11 block of the Yinggehai Basin, the South China Sea. *Mar. Pet. Geol.* **2018**, *97*, 49–65. [[CrossRef](#)]
59. Yang, T.; Cao, Y.; Friis, H.; Liu, K.; Wang, Y.; Zhou, L.; Yuan, G.; Xi, K.; Zhang, S. Diagenesis and reservoir quality of lacustrine deep-water gravity-flow sandstones in the Eocene Shahejie Formation in the Dongying sag, Jiyang depression, eastern China. *Am. Assoc. Pet. Geol. Bull.* **2020**, *104*, 1045–1073. [[CrossRef](#)]
60. Wang, X.; Wei, H.; Shi, W.; Wang, Y. Formation pressure characteristics and hydrocarbon accumulation in eastern Kuqa Depression. *Geol. Sci. Technol. Inf.* **2016**, *35*, 68–73.
61. Ju, Y.; Sun, X.; Liu, L.; Xie, Y.; Wei, H. Characteristics of Jurassic Tight Sandstone Gas Reservoir in Dibe Area of Kuqa Depression, Tarim Basin. *Xinjiang Pet. Geol.* **2014**, *35*, 264–267.
62. Yue, D.; Wu, S.; Xu, Z.; Xiong, L.; Chen, D.; Ji, Y.; Zhou, Y. Reservoir quality, natural fractures, and gas productivity of upper Triassic Xujiahe tight gas sandstones in western Sichuan Basin, China. *Mar. Pet. Geol.* **2018**, *89*, 370–386. [[CrossRef](#)]
63. Tokan-Lawal, A.; Prodanovic, M.; Eichhubl, P. Investigating flow properties of partially cemented fractures in Travis Peak Formation using image-based pore-scale modeling. *J. Geophys. Res. Solid Earth.* **2015**, *120*, 5453–5466. [[CrossRef](#)]
64. Lu, X.; Zhao, M.; Liu, K.; Zhuo, Q.; Fan, J.; Yu, Z.; Gong, Y. Forming condition and mechanism of highly effective deep tight sandstone gas reservoir in Kuqa foreland basin. *Acta Pet. Sin.* **2018**, *39*, 365–378.
65. Li, J.; Wang, C.; Li, J.; Ma, W.; Zhang, H.; Lu, Y.; Li, D.; Liu, M. Source and exploration direction of tight oil and gas in the Dibe section of northern Kuqa Depression. *China Pet. Explor.* **2019**, *24*, 485–497.
66. Wei, G.; Zhang, R.; Zhi, F.; Wang, K.; Yu, C.; Dong, C. Formation conditions and exploration directions of Mesozoic structural lithologic stratigraphic reservoirs in the eastern Kuqa Depression. *Acta Pet. Sin.* **2021**, *42*, 1113–1125.